On the Stability of Shield-Driver Circuits

Enrique Mario Spinelli, *Senior Member, IEEE*, and Ferran Reverter

Abstract—This paper analyzes the stability of shield-driver circuits (SDCs) applied to the measurement of remote signal sources (such as bioelectric signals) and then proposes design ideas to guarantee it. According to the performed analysis, there are at least two factors that explain the potential instability of the SDC: 1) a high order of the SDC transfer function and 2) the parasitic inductance of the interconnecting cable. The former makes the circuit unstable for intermediate values of the output resistance R_S of the signal source, whereas the latter makes the circuit unstable for low values of R_S. These theoretical predictions are experimentally validated using several commercial operational amplifiers.

Index Terms—Active shielding, shield-driver circuit (SDC), shielded cable, stability.

I. INTRODUCTION

R EMOTE sensors and signal sources are usually connected to their electronics via shielded cables to reduce the effects of electric field interference. The common practice is to connect the cable shield to the ground potential, which is called passive shielding. However, this configuration is not useful in some applications due to the effects of the parasitic capacitance C_{SH} of the cable. This capacitance considerably increases the parasitic capacitance to ground, and hence, passive shielding becomes inappropriate for the measurement of grounded capacitive sensors [1], [2] or the characterization of voltmeter input parameters [3]. The capacitance C_{SH} also decreases the effective input impedance of the readout circuit and can bring about phase and gain errors, which can be a major problem, for example, in impedance measurements [4], [5]. Another effect caused by C_{SH} is the reduction of the effective common-mode rejection ratio of differential amplifiers, as can happen, for instance, in the measurement of bioelectric signals [6].

The usual way to avoid the previous effects while preserving shielding effectiveness is by applying active shielding, i.e., driving the cable shield at the same potential as that of the inner conductor by using a shield-driver circuit (SDC), as shown in Fig. 1. In this configuration, external interferences are driven to ground through the low output impedance of the SDC, and
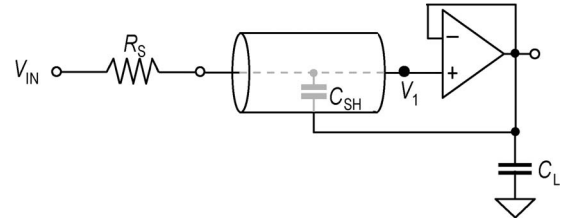
E. M. Spinelli is with the Industrial Electronics, Control, and Instrumentation Laboratory (LEICI), Facultad de Ingeniería, Universidad Nacional de La Plata (UNLP)–Consejo de Investigaciones Científicas y Técnicas (CONICET), 1900 La Plata, Argentina (e-mail: spinelli@ing.unlp.edu.ar).

F. Reverter is with the Instrumentation, Sensors and Interfaces Group, Castelldefels School of Technology (EPSC), Technical University of Catalonia (UPC), 08860 Castelldefels, Spain (e-mail: reverter@eel.upc.edu).

Fig. 1. Measurement of a remote signal source by applying active shielding.

C_{SH} ideally does not affect the measurement because both cable conductors are at the same potential. However, active shielding has problems in terms of "electronic" instability due to the positive feedback path generated by C_{SH} [7]. Instability problems are generally solved by means of practical pieces of advice such as decreasing a little bit the gain (e.g., 0.99) of the SDC [5], [6].

To the best of our knowledge, few papers have theoretically analyzed the stability of SDCs. For the measurement of grounded capacitive sensors, stability was carefully analyzed in [8]. For the measurement of bioelectric signals, stability was analyzed in [6]; however, such an analysis used simple circuit models, and no effects of the source impedance on the stability were predicted. This paper improves the approach proposed in [6] and analyzes in detail the stability of SDCs when measuring voltage-modulated signal sources, such as bioelectric signals, or the voltage resulting from impedance measurements.

II. CIRCUIT ANALYSIS

Fig. 1 shows an SDC intended for the measurement of a remote signal source, which is modeled by the voltage source V_{IN} and the resistance R_S; the output impedance of the signal source is assumed to be only a resistance to simplify the analysis [6]. The SDC is implemented by an operational amplifier (OpAmp) configured as a unity–gain buffer and drives the cable shield to the same potential as that of the inner conductor. The capacitance C_{SH} is the parasitic capacitance between the inner conductor and the shield of the interconnecting cable; note that a positive feedback path is established through C_{SH}, which could lead to instability problems. The capacitance C_L is the capacitive load of the buffer. When a triaxial cable is used and the second shield is connected to ground to be the current return path, C_L is almost equal to the parasitic capacitance C_{SS} between the first and the second shield of the cable.

The circuit in Fig. 1 can be analyzed by the equivalent circuit in Fig. 2, in which $G(s)$ is the transfer function of the buffer when driving the capacitive load C_L. Let us first assume that $G(s)$ is a first-order low-pass transfer function [6], i.e.,

$$G(s) = \frac{1}{1 + s\tau_1} \qquad (1)$$

Fig. 2. Equivalent circuit of the circuit shown in Fig. 1.

Fig. 3. Equivalent circuit of the circuit shown in Fig. 1 when the input capacitance of the OpAmp is considered.

where τ_1 is the time constant of the buffer and is equal to $1/\omega_1$, ω_1 being the bandwidth of the buffer in radians per second. Accordingly, the circuit in Fig. 2 has the following transfer function:

$$T(s) = \frac{V_1(s)}{V_{\text{IN}}(s)} = \frac{s + \omega_1}{s^2 \tau_G + s + \omega_1} \quad (2)$$

where $\tau_G = R_S C_{\text{SH}}$. The characteristic polynomial of (2) is of the second order and has positive coefficients. Therefore, its roots have a negative real part [9], and the circuit should be stable for any value of R_S, C_{SH}, and ω_1 [6].

Practice with the SDC shows instability problems, and this means that the models used before are not good enough to foresee the circuit stability. For this reason, the following sections again analyze the circuit using improved models of both the buffer and the cable. The effects of these improved models are separately evaluated because a simultaneous analysis results in complex analytical expressions that are useless for a conceptual interpretation of the different factors involved. The stability condition resulting from each particular analysis does not completely ensure stability since it results from a noncomplete model of the circuit. The circuit will be stable only when both stability conditions are fulfilled.

A. Transfer Function of the Buffer

When the buffer drives a high capacitive load C_L, its transient response significantly differs from the first-order response previously assumed. For this reason, we proceed to analyze the circuit when $G(s)$ is a second-order transfer function, i.e.,

$$G(s) = \frac{\omega_2^2}{s^2 + 2\xi_2 \omega_2 s + \omega_2^2} \quad (3)$$

where ω_2 is the undamped natural frequency, and ξ_2 is the damping ratio. These parameters depend on the OpAmp features and also on the capacitive load, which is almost equal to the parasitic capacitance C_{SS} of the cable. Consequently, since C_{SS} depends on the cable length, then $G(s)$ also depends on the cable length. The effects of the input capacitance C_{IN} of the OpAmp are also considered here, as shown in Fig. 3.

Using (3), the circuit in Fig. 3 has the transfer function $T(s)$ in (4), shown at the bottom of the page, where $\tau_i = R_S C_{\text{IN}}$.
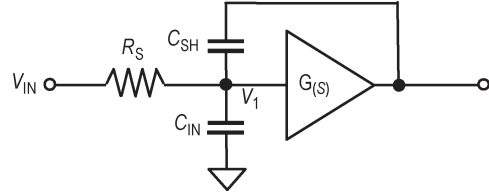
Considering that $\tau_i \ll \tau_G$, the characteristic polynomial of (4) can be simplified to

$$s^3 \tau_G + s^2 (2\xi_2 \omega_2 \tau_G + 1) + s \left(\omega_2^2 \tau_i + 2\xi_2 \omega_2 \right) + \omega_2^2. \quad (5)$$

Applying the Routh–Hurwitz stability criterion [9] in (5) and assuming $C_{\text{IN}} \ll C_{\text{SH}}$, the stability condition is

$$4\xi_2^2 + 2\xi_2 \left(\omega_2 R_S C_{\text{IN}} + \frac{1}{\omega_2 R_S C_{\text{SH}}} \right) > 1. \quad (6)$$

According to (6), stability depends on several parameters. High values of ξ_2 and low values of C_{SH} are recommended to ensure stability. Stability could also be improved by using a high value of C_{IN}, but this is not appropriate because the purpose of the SDC is to keep the input capacitance to ground low. Stability also depends on the values of R_S and ω_2 so that the circuit is stable for low and high values of R_S and ω_2, but not for intermediate values. For instance, Fig. 4 shows the function f of R_S, i.e.,

$$f(R_S) = 4\xi_2^2 + 2\xi_2 \left(\omega_2 R_S C_{\text{IN}} + \frac{1}{\omega_2 R_S C_{\text{SH}}} \right) \quad (7)$$

which points out that the circuit is stable (i.e., $f(R_S) > 1$) for $R_S < R_{S,A}$ and $R_S > R_{S,B}$, but not for intermediate values. This dependence on the value of R_S can be critical in those applications where R_S is not constant, for example, in biopotential measurements [10] and impedance tomography [11].

From (7), we can determine the minimum value of f (i.e., f_{min}) and the value of R_S (i.e., $R_{S,C}$) that brings about f_{min} (Fig. 4), i.e.,

$$R_{S,C} = \frac{1}{\omega_2 \sqrt{C_{\text{IN}} C_{\text{SH}}}} \quad (8)$$

$$f_{\text{min}} = f(R_{S,C}) = 4\xi_2^2 + 4\xi_2 \sqrt{C_{\text{IN}}/C_{\text{SH}}}. \quad (9)$$

From (6) and (7), the circuit is clearly stable if f_{min} is greater than 1. The parameter f_{min} depends on the ratio $C_{\text{IN}}/C_{\text{SH}}$, but this is quite variable since C_{SH} depends on the cable type and length and C_{IN} depends on the OpAmp used. Therefore, a good option to ensure the stability of the circuit (i.e., $f_{\text{min}} > 1$) for any ratio $C_{\text{IN}}/C_{\text{SH}}$ is to select a buffer with $4\xi_2^2$ higher than 1

$$T(s) = \frac{V_1(s)}{V_{\text{IN}}(s)} = \frac{s^2 + 2\xi_2 \omega_2 s + \omega_2^2}{s^3 (\tau_i + \tau_G) + s^2 \left[2\xi_2 \omega_2 (\tau_i + \tau_G) + 1 \right] + s \left(\omega_2^2 \tau_i + 2\xi_2 \omega_2 \right) + \omega_2^2} \quad (4)$$
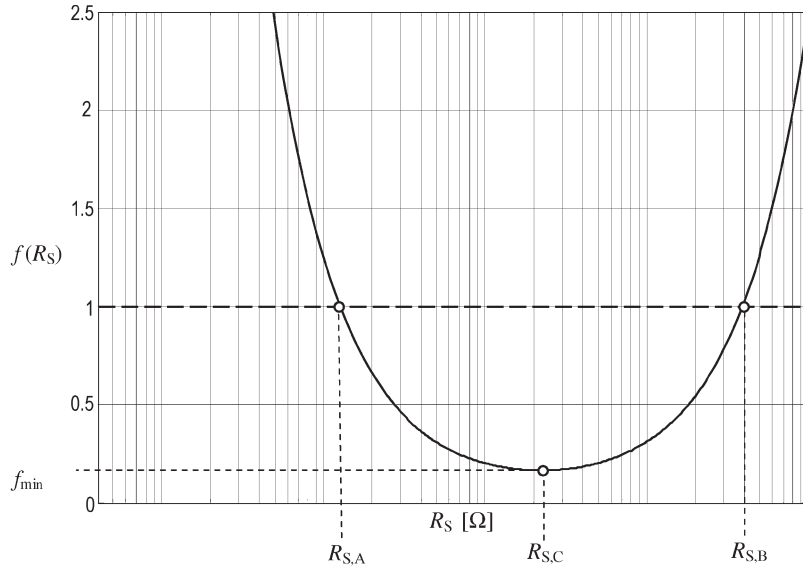
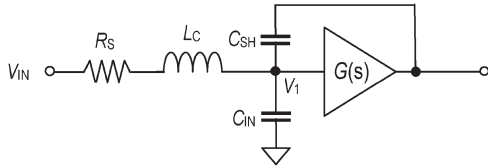Fig. 4.   Typical response of the function $f(R_S)$ described by (7).

Fig. 5.   Equivalent circuit of the circuit shown in Fig. 1 when the cable inductance is considered.

or, in other words, ξ_2 higher than 0.5. Note that the buffer must have this damping ratio when driving the capacitive load C_L. For this reason, it is advisable to select an OpAmp able to drive high-value capacitive loads and/or to apply appropriate compensation methods, for example, adding a resistor (either out or in the loop) between the OpAmp output and the capacitive load [12].

Once the stability of the SDC is guaranteed, the next issue to analyze is the transient response of the voltage at node V_1. Although this analysis is not the main objective of this paper, next, we provide some comments about it. The transient response can be found from (4), but there are not simple relationships between the parameters of the circuit and the features of the transient response. However, according to simulations, the step transient response is underdamped when R_S is close to the critical values $R_{S,A}$ and $R_{S,B}$ (Fig. 4), whereas it becomes more damped as R_S decreases with respect to $R_{S,A}$ or increases with respect to $R_{S,B}$. In addition, the higher the value of R_S, the slower the transient response.

B. Cable Inductance

In the previous analyses (Figs. 2 and 3), the interconnecting cable was modeled only with a lumped capacitor C_{SH}. This electric model, however, is not accurate enough for stability analysis, particularly when long cables are used. Such a model can be improved by adding the inductance L_C of the current loop between the signal source and the readout circuit, as shown in Fig. 5. A lumped model is considered for the inductance

to simplify the analysis and because it was already used and experimentally verified in [8].

The following analysis takes into account the effects of L_C but assumes a first-order $G(s)$ to keep a low-complexity model, as explained at the beginning of Section II. Then, assuming (1) and some practical relations between parameters (e.g., $\tau_i \ll \tau_G$ and $C_{IN} \ll C_{SH}$), the transfer function of the circuit in Fig. 5 can be approximated to

$$T(s) = \frac{V_1(s)}{V_{IN}(s)} \approx \frac{s + \omega_1}{s^3 L_C C_{SH} + s^2 \tau_G + s(\omega_1 \tau_i + 1) + \omega_1}.$$
(10)

Applying the Routh–Hurwitz stability criterion [9] to the characteristic polynomial of (10), the stability condition is

$$\frac{R_S}{\omega_1} + R_S^2 C_{IN} > L_C$$
(11)

which shows that high values of R_S are appropriate to guarantee stability. For low values of R_S and typical values for the rest of parameters, the first term on the left side of (11) predominates over the second term, and then, the stability condition can be simplified to

$$R_S > \omega_1 L_C.$$
(12)

According to (12), the circuit becomes unstable for low values of R_S, particularly when high-bandwidth OpAmps (i.e., a large ω_1) and long cables (i.e., a large L_C) are used. For example, for $\omega_1 = 2\pi \cdot 20$ MHz and $L_C = 2$ μH, the stability condition is $R_S > 251$ Ω. Therefore, high-bandwidth OpAmps are not advisable when using long interconnecting cables.

III. EXPERIMENTAL RESULTS AND DISCUSSION

The stability models developed in Section II were validated by means of the experimental setup shown in Fig. 6. A battery of 1.5 V was used as a signal source; this battery also provided
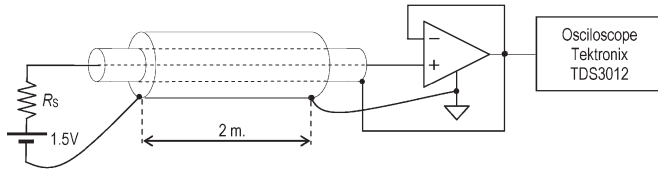
Fig. 6. Experimental setup to validate the stability models developed in Section II.

TABLE I
EXPERIMENTAL VALUES OF THE PARAMETERS C_{IN}, ω_2, AND ξ_2 OF THE
UNITY–GAIN BUFFER WHEN DRIVING A CAPACITIVE LOAD
$C_{SS} = 720$ pF

	LM358	TLC2202	OPA350	OP07
C_{IN} (pF)	3	22	7	7
ω_2 (rad/s)	$2\pi \cdot 480$k	$2\pi \cdot 900$k	$2\pi \cdot 14$M	$2\pi \cdot 800$k
ξ_2	0.08	0.15	0.3	0.55

a dc level to ensure a linear operation for the single-supply OpAmps. A resistor R_S (ranging from 10 Ω to 1 MΩ) emulated the output resistance of the signal source. Then, the signal was connected to the circuit through a 2-m triaxial cable. This cable was characterized by an impedance analyzer (HP4262A), and the results were $C_{SH} = 192$ pF, $C_{SS} = 720$ pF, and $L_C = 0.8$ μH. The first shield of the cable was driven by a unity–gain buffer implemented by different commercial OpAmps (LM358, TLC2202, OPA350, and OP07). The second shield was connected to ground, and hence, the capacitive load C_L of the buffer was almost equal to C_{SS}. The OpAmps operated at a single supply voltage (5 V) except for OP07, which operated at ± 15 V. The output voltage of the buffer was connected to a digital oscilloscope (Tektronix TDS3012) to display the state (i.e., stable or unstable) of the circuit.

Table I summarizes the experimental values of C_{IN}, ω_2, and ξ_2 for each tested OpAmp. The parameters ω_2 and ξ_2 were estimated by applying a step of 10 mV at the input of the unity–gain buffer and approximating a second-order response to the output transient response when driving a capacitive load of 720 pF. Using the values in Table I and (7), we calculated the theoretical functions $f(R_S)$ for the four OpAmps, which are represented in Fig. 7. According to Fig. 7, the circuit should be unstable (i.e., $f(R_S) < 1$) for the following intermediate values of R_S: between 280 Ω and 670 kΩ for LM358, between 300 Ω and 24 kΩ for TLC2202, and between 60 and 1700 Ω for OPA350; OP07 should be always stable since $\xi_2 > 0.5$.

Using (12), we calculated the theoretical minimum value of R_S ($R_{S,min}$) to guarantee stability in terms of cable inductance effects. The value of ω_1 considered to calculate $R_{S,min}$ was the experimental value of ω_2 shown in Table I; it is true that ω_2 corresponds to a second-order response, but it is the best estimation of the buffer bandwidth that we have, particularly when driving a high-value capacitive load. For LM358, TLC2202, and OP07, $R_{S,min}$ was lower than 5 Ω, which means that cable inductance effects are almost negligible in terms of stability. However, for OPA350, $R_{S,min} = 70$ Ω, and therefore, if we
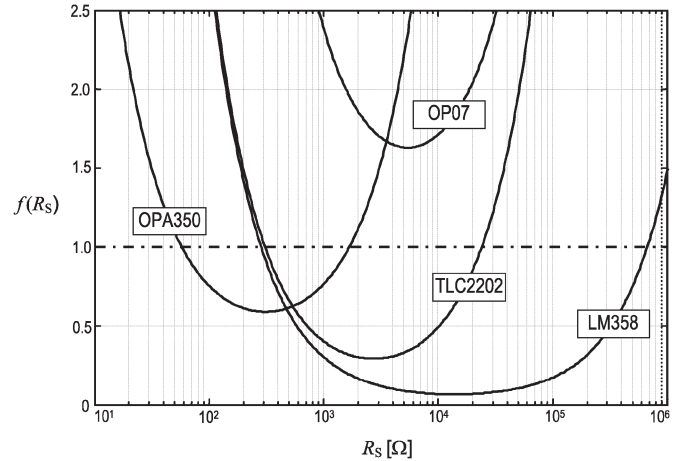

Fig. 7. Function $f(R_S)$ described by (7) for the tested OpAmps.

TABLE II
EXPERIMENTAL RESULTS OF THE STABILITY TESTS FOR
DIFFERENT VALUES OF R_S

R_S (Ω)	LM358	TLC2202	OPA350	OP07
10	Stable	Stable	Unstable	Stable
50	Stable	Stable	Unstable	Stable
100	Stable	Stable	Unstable	Stable
1 k	Unstable	Unstable	Unstable	Stable
10 k	Unstable	Unstable	Stable	Stable
100 k	Unstable	Stable	Stable	Stable
1 M	Stable	Stable	Stable	Stable

take into account both stability conditions, the circuit should be unstable for $R_S < 1700$ Ω.

Table II shows the experimental results of the stability tests for the different values of R_S and for each tested OpAmp. LM358 and TLC2202 were unstable only for intermediate values of R_S, as predicted in the last paragraph. OPA350 was unstable for low and intermediate values of R_S, which also agrees with the theoretical predictions. Finally, OP07 was always stable for the values of tested R_S, which was also predicted before. Therefore, the fact of considering a second-order response for the buffer and the cable inductance seem to be key points to foresee the circuit stability.

IV. CONCLUSION

Stability of SDCs depends on the OpAmp's response working as a unity–gain buffer, the output resistance R_S of the signal source, and the cable parameters. Due to the high order of the transfer function of the buffer, the circuit becomes unstable for intermediate values of R_S. A unity–gain buffer with a damping ratio greater than 0.5 avoids such instability problems. On the other hand, due to the parasitic inductance of the interconnecting cable, the circuit becomes unstable for low values of R_S. To prevent such effects, it is advisable not

to select a high-bandwidth OpAmp when using long cables. All these theoretical stability conditions have experimentally been verified for different commercial OpAmps.

ACKNOWLEDGMENT

REFERENCES

[1] S. M. Huang, A. L. Stott, R. G. Green, and M. S. Beck, "Electronic transducers for industrial measurement of low value capacitances," *J. Phys. E, Sci. Instrum.*, vol. 21, no. 3, pp. 242–250, Mar. 1988.

[2] D. Marioli, E. Sardini, and A. Taroni, "High-accuracy measurement techniques for capacitance transducers," *Meas. Sci. Technol.*, vol. 4, no. 3, pp. 337–343, Mar. 1993.

[3] I. Lenicek, D. Ilic, and R. Malaric, "Determination of high-resolution digital voltmeter input parameters," *IEEE Trans. Instrum. Meas.*, vol. 57, no. 8, pp. 1685–1688, Aug. 2008.

[4] B. P. Iliev, G. A. M. Pop, and G. C. M. Meijer, "In-vivo blood characterization system," in *Proc. IEEE IMTC*, Apr. 2006, pp. 1781–1785.

[5] H. G. Goovaerts, T. J. C. Faes, E. Raaijmakers, and R. M. Heethaar, "Some design concepts for electrical impedance measurement," *Ann. N.Y. Acad. Sci.*, vol. 873, no. 1, pp. 388–395, Apr. 1999.

[6] A. C. Meeting van Rijn, A. Peper, and C. A. Grimbergen, "High-quality recording of bioelectric events. Part 1: Interference reduction, theory and practice," *Med. Biol. Eng. Comput.*, vol. 28, no. 5, pp. 389–397, Sep. 1990.

[7] R. Morrison, *Solving Interference Problems in Electronics*. New York: Wiley, 1995.

[8] F. Reverter, X. Li, and G. C. M. Meijer, "Stability and accuracy of active shielding for grounded capacitive sensors," *Meas. Sci. Technol.*, vol. 17, no. 11, pp. 2884–2890, Nov. 2006.

[9] R. C. Dorf and R. H. Bishop, *Modern Control Systems*. Upper Saddle River, NJ: Prentice–Hall, 2005.

[10] J. Rosell, J. Colominas, P. Riu, R. Pallàs-Areny, and J. G. Webster, "Skin impedance from 1 Hz to 1 MHz," *IEEE Trans. Biomed. Eng.*, vol. 35, no. 8, pp. 649–651, Aug. 1988.

[11] D. S. Holder, *Electrical Impedance Tomography: Methods, History and Applications*. Bristol, U.K.: CRC Press, 2005.

[12] *Operational amplifier stability compensation methods for capacitive loading applied to TS507*, STMicroelectronics, Geneva, Switzerland, 2007. [Online]. Available: http://www.st.com

Enrique Mario Spinelli (S'98–M'02–SM'08) was born in Balcarce, Argentina, in 1964. He received the Engineer degree in electronics and the M.S. and Ph.D. degrees from the Universidad Nacional de La Plata (UNLP), La Plata, Argentina, in 1989, 2000, and 2005, respectively.

Since 1990, he has been with the Industrial Electronics, Control, and Instrumentation Laboratory (LEICI), Facultad de Ingeniería, UNLP, working on scientific instrumentation. He is currently a Professor of control systems with the Facultad de Ingeniería, UNLP, and a Researcher with the Consejo Nacional de Investigaciones Científicas y Técnicas (CONICET). His current research interests are analog signal processing and brain control interfaces.

Ferran Reverter was born in Llagostera, Spain, on January 4, 1976. He received the B.Sc. degree in industrial electronic engineering from the University of Girona, Girona, Spain, in 1998, the M.Sc. degree in electronic engineering from the University of Barcelona, Barcelona, Spain, in 2001, and the Ph.D. degree in electronic engineering from the Technical University of Catalonia (UPC), Barcelona, in 2004.

Since 2001, he has been an Assistant Professor of analogue electronics and digital systems with the UPC. From 2005 to 2007, he was a Visiting Postdoctoral Fellow with Delft University of Technology, Delft, The Netherlands. He is the coauthor (with R. Pallàs-Areny) of the book *Direct Sensor-to-Microcontroller Interface Circuits* (Barcelona: Marcombo, 2005). His research interests are in the field of electronic instrumentation, particularly the design and characterization of interface circuits for sensors.